

P40 and TTF-1 double-expressing non-small cell lung cancer with EML4-ALK and PIK3CA gene mutations: A case report and review of the literature

YING CAI¹, HONGSHENG LIU², XIAODAN CHEN², JUNJIE YANG² and BIN HUANG²

Departments of ¹Respiratory Medicine and ²Pathology,
The First People's Hospital of Xiaoshan District, Hangzhou, Zhejiang 311200, P.R. China

Received August 19, 2022; Accepted December 7, 2022

DOI: 10.3892/ol.2022.13645

Abstract. P40 and thyroid transcription factor-1 (TTF-1) dual expression in non-small cell lung cancer (NSCLC) is a rare occurrence. However, the presence of EML4-ALK and PIK3CA gene mutations in this type of cancer is unknown. The present study describes the case of a 38-year-old male patient who had never smoked. A 4.5-cm mass adjacent to his right upper mediastinum was detected by a computed tomography (CT) scan of the chest. Biopsy of the level four lymph nodes in the right mediastinum revealed microscopic morphological features typical of high-grade NSCLC. Immunohistochemical findings resembled those reported previously for several cases of NSCLC with the dual expression of P40 and TTF-1 markers. In addition, echinoderm microtubule-associated protein-like 4-anaplastic lymphoma kinase (EML4-ALK) and phosphatidylinositol-4,5-bisphosphate 3-kinase catalytic subunit a (PIK3CA) gene mutations were detected using high-throughput next-generation sequencing. To the best of our knowledge, this is the first report of NSCLC with the expression of P40 and TTF-1 as well as EML4-ALK and PIK3CA gene mutations. The presence of this type of tumor should be considered in patients with NSCLC who have never smoked and may have unique clinicopathological features.

Introduction

The first study on non-small cell lung cancer (NSCLC) with the double expression of P40 and thyroid transcription factor-1 (TTF-1) was reported by Pelosi *et al* (1) in 2015. Since then, only a few studies on this topic have been published (2-5). In these studies, immunohistochemistry (IHC) revealed the

expression of P40 and TTF-1 in the same tumor cells, while the ultrastructural examination of the cells showed adenoid and squamous differentiation characteristics (1,4). The histological features were consistent with those of NSCLC. In all cases, the high-grade tumor cells presented in solid nests with a lamellar distribution, and exhibited distinct atypia, a high nucleoplasmic ratio and mitotic figures; some were necrotic and some exhibited squamous differentiation, adenoid differentiation and peripheral palisade structures. The gene mutations accompanying this disease vary; all six reported cases had a TP53 mutation or genetic polymorphism, including epidermal growth factor receptor gene (EGFR) (4), KRAS (1), PTEN (2) and neurofibromin 1 (NF1) (4) mutations, and fibroblast growth factor receptor 1 (FGFR1) (1) amplification with programmed death ligand 1 (PD-L1) (3) expression. Treatments administered include surgery, radiotherapy, chemotherapy and targeted therapy, the effects of which were inconsistent.

The present article documents a case of lung adenosquamous carcinoma (LASC), a subtype of NSCLC with P40 and TTF-1 double expression and echinoderm microtubule-associated protein-like 4-anaplastic lymphoma kinase (EML4-ALK) and phosphatidylinositol-4,5-bisphosphate 3-kinase catalytic subunit a (PIK3CA) gene mutations. This case highlights that this tumor cell can exhibit the characteristics of adenosquamous differentiation at the cytological level, which differs from the current definition of LASC recommended by the World Health Organization (WHO) (6).

Case report

A 38-year-old male patient with no history of smoking was admitted to the First People's Hospital of Xiaoshan District (Hangzhou, China) on June 24, 2019 with a cough and expectoration that had persisted for 4 months and become aggravated during the last month. On physical examination post-admission, the patient had a respiratory rate of 18 breaths/min and the lymph nodes on both sides of the clavicle were palpable; the larger nodes were approximately the size of a pea. A chest computed tomography (CT) scan showed a right mediastinal mass 4.5x3.7 cm in size (Fig. 1). Mediastinal lung cancer with superior vena cava invasion was considered as a potential

Correspondence to: Dr Bin Huang, Department of Pathology, The First People's Hospital of Xiaoshan District, 199 Shixin South Road, Xiaoshan, Hangzhou, Zhejiang 311200, P.R. China
E-mail: h740925@sina.com

Key words: P40, TTF-1, double expression, EML4-ALK, PIK3CA, mutation, lung cancer

diagnosis. The patient had multiple nodules and patchy shadows in both lungs, numerous enlarged lymph nodes in the mediastinum, right hilum and bilateral supraclavicular region, but no pleural effusion. Multiple ribs, thoracic vertebrae, scapula bone density abnormalities and osteogenic metastases were considered. The serological tumor markers were as follows: Carcinoembryonic antigen 9.20 $\mu\text{g/l}$ (normal range, 0.00-5.00 $\mu\text{g/l}$), cytokeratin 19 fragment 5.15 ng/ml (normal range, <3.3 ng/ml), cancer antigen (CA) 125 30.80 kU/l (normal range, <35 kU/l), CA199 <2.00 kU/l (normal range, <37 kU/l) and squamous cell carcinoma-associated antigen 1.30 $\mu\text{g/l}$ (normal range <1.5 $\mu\text{g/l}$). Transbronchial endoscopic ultrasound was employed to perform a biopsy of the level four mediastinal lymph nodes. Cytopathologic investigation of the right supraclavicular lymph nodes was performed using fine needle aspiration. Gross pathological examination of the biopsy of the right level four mediastinal lymph node revealed a large mass of broken tissues that was gray, white and red in color ($\sim 1.0 \times 0.8 \times 0.3 \text{ cm}^3$). The tissues were fixed with 4% neutral buffered formalin (24 h at 25°C) and paraffinized to prepare 4- μm sections for hematoxylin and eosin staining (according to a standard protocol) and IHC staining. High-throughput next-generation sequencing (NGS) was employed to detect the molecular pathology.

Microscopic examination of the tissues at low power revealed that the broken tumor tissue was distributed in clusters and nests (Fig. 2), and a small number of lymphocytes were present in a loose cellulose exudate between tumor nests without evident fibrous stroma. At high magnification, solid flake tumor cells were observed with obvious cell atypia, different cell sizes and clear boundaries in some parts. In addition, the cells had a high nucleus-plasma ratio, varying nuclear sizes, coarse chromatin and indistinct nucleoli. Mitotic figures were visible, along with abundant eosinophilic cytoplasm and some nuclear deviation. However, no salt and pepper-like particles, keratinization or necrosis were observed (Fig. 3).

IHC was performed using an EnVision IHC kit (polymer method; cat. no. KIT-0014; Beijing Jinqiao Zhongshan Biological Co. Ltd.) with antibodies from Beijing Zhongshan Jinqiao Biological Co., Ltd. to target the following proteins (pre-diluted working solutions unless otherwise indicated): P40 (cat. no. 2106230815d), TTF-1 (cat. no. 2011260599c7), cytokeratin (CK)7 (cat. no. 21050820), napsin A (cat. no. 21110130), Ki-67 (1:200 dilution; cat. no. 21030436), P63 (cat. no. 21063006), CD56 (cat. no. 21082702), chromogranin A (CgA; cat. no. 2108052), synaptophysin (Syn; cat. no. 2105130742c), CK5/6 (cat. no. 21030108), paired box 8 (Pax8; cat. no. 21012350), thyroglobulin (TG; cat. no. 20030932) and Tp53 (cat. no. 20082125). The results were as follows: P40 50-60%+ (Fig. 4), TTF-1+ (Fig. 5), CK7+ (Fig. 6) and napsin A+ (Fig. 7). In addition, the Ki-67 proliferation index was 10% positive, P63, CD56, CgA, Syn, CK5/6, Pax8 and TG staining were negative; and TP53 exhibited no mutations.

Molecular pathology. For this analysis, 15 paraffin sections were extracted and library construction and probe capture were performed (AmoyDx Essential NGS Panel; cat. no. 8.0627401X0241; Amoy Diagnostics Co., Ltd.). High-throughput NGS was performed to detect gene mutations associated with drug sensitivity in the solid tumor sections. The

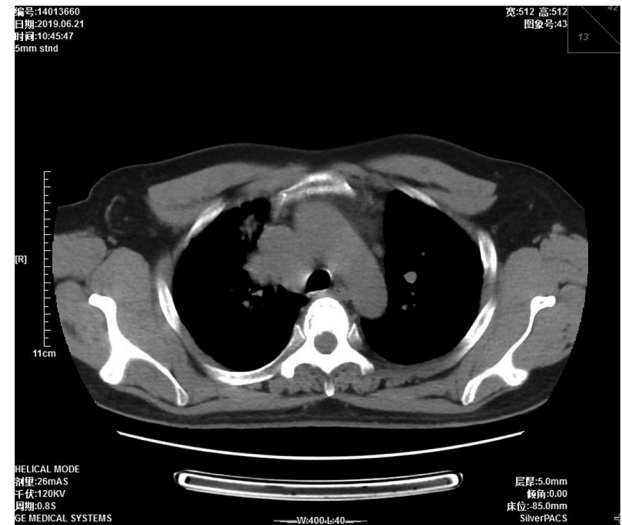


Figure 1. Prior to treatment, computed tomography showed a mass in the right upper mediastinum with a size of 4.5x3.7 cm. Mediastinal lung cancer was considered.

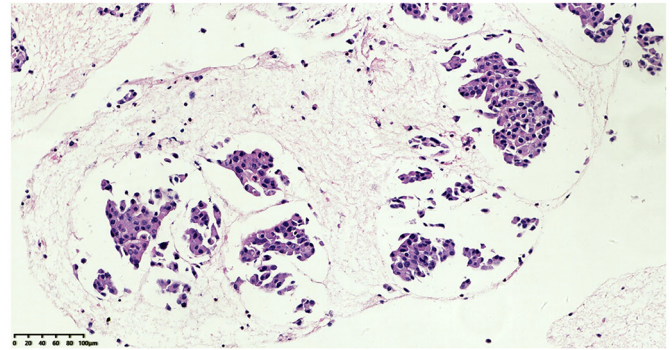


Figure 2. Microscopic examination revealed that the tumor tissue was distributed in clumps and nests. Hematoxylin and eosin staining (scale bar, 100 μm).

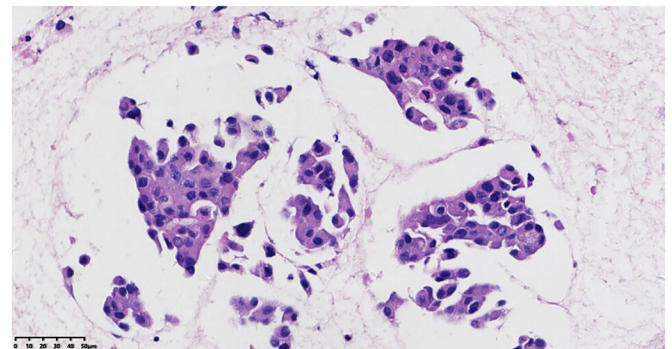


Figure 3. Tumor tissue observed at high magnification. The tumor cells exhibited obvious atypia, a high nucleoplasmic ratio, variably sized nuclei, coarse chromatin, inconspicuous nucleoli and abundant eosinophilic cytoplasm. In addition, some nuclei were skewed, and appeared to have an adenoid structure. Hematoxylin and eosin staining (scale bar, 50 μm).

reagent used was a 10-gene kit procured from Amoy Diagnostics Co., Ltd. A sequencing platform from Illumina, Inc. was used with a cancer gene mutation information analysis system developed by Amoy Diagnostics Co., Ltd., as the analytical software.

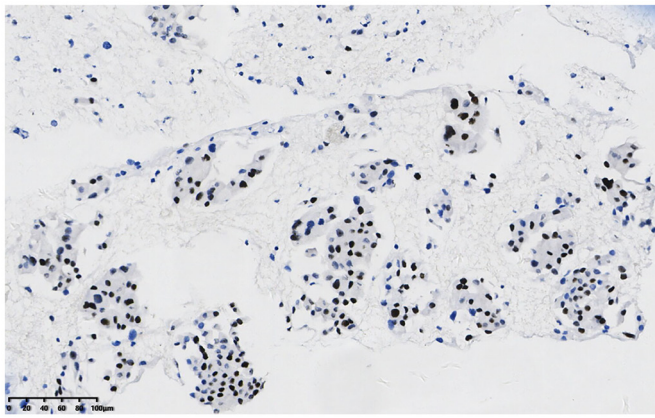


Figure 4. Immunohistochemical staining revealed that the tumor cells were 50-60% positive for P40 (scale bar, 100 μ m).

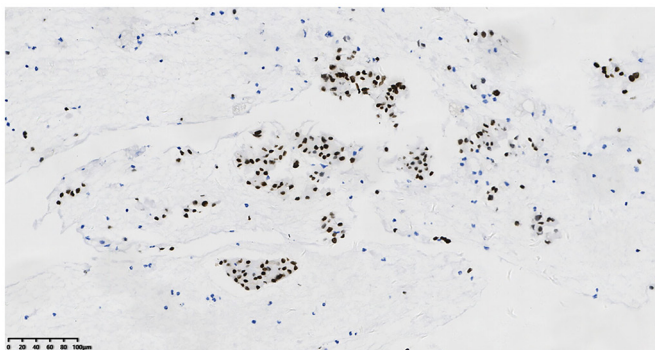


Figure 5. Immunohistochemical staining revealed that the tumor cells were strongly positive for thyroid transcription factor-1 (scale bar, 100 μ m).

Molecular pathology results and drug sensitivity. The mutation rate was 24.77% for the fusion gene between exon 6 of EML4 and exon 20 of ALK (ALK transcript NM_004304.4 and EML4 transcript NM_019063.4; indel fusion), and according to US Food and Drug Association/National Comprehensive Cancer Network guidelines, this mutation indicates that the tumor is sensitive to crizotinib (www.nccn.org/patients). The mutation rate of the PIK3CA gene was 4.32% (exon10 c.1658 G>C p.S553t, transcript NM_0062182, mutation type single nucleotide variant; indel), suggesting a lack of drug sensitivity, and resistance to gefitinib, erlotinib, afatinib and icotinib. No mutations were observed in EGFR, BRAF, HER2, KRAS, MET, ROS1, RET and NRAS genes.

Pathological diagnosis. The patient presented with lymph node metastatic poorly differentiated carcinoma, combined with a clinical diagnosis of NSCLC with P40 and TTF-1 expression and EML4-ALK and PIK3CA gene mutations. Fine needle aspiration cytology of the right supraclavicular lymph node revealed poorly differentiated cancer cells. The clinical stage was cT3N3M1c-stage IVB.

Treatment and follow-up. In July 2019, 850 mg pemetrexed combined with 600 mg carboplatin was started daily as intravenous chemotherapy. Due to abnormal liver function, the patient stopped chemotherapy immediately after the first

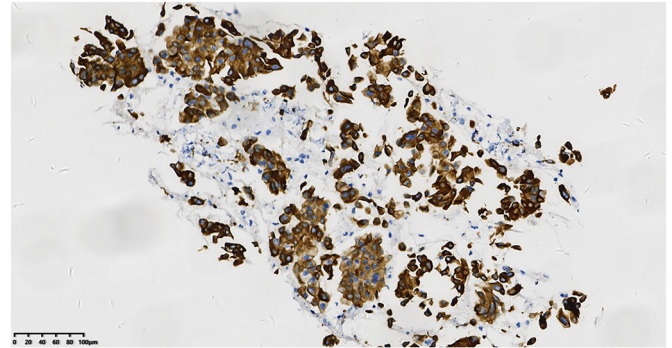


Figure 6. Immunohistochemical staining of the tumor cells was strongly positive for cytokeratin 7 (scale bar, 100 μ m).

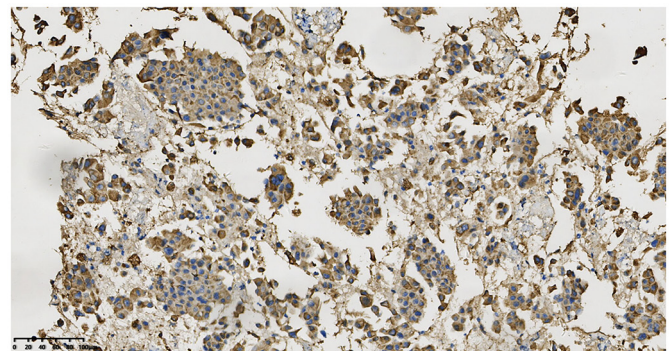


Figure 7. Immunohistochemical staining of the tumor cells was strongly positive for napsin A (scale bar, 100 μ m).

chemotherapy cycle, and then began single-agent targeted therapy with 250-mg oral crizotinib capsules 8 days after starting intravenous chemotherapy. The tumor shrank by ~50% within 1 month on CT (Fig. 8). After 3 months, the lung tumor had shrunk further on CT (Fig. 9). The patient was subsequently lost to follow-up.

Discussion

In the GLOBOCAN 2020 estimates reported by Sung *et al* (7) for 36 types of cancer in 185 countries, the incidence and mortality of lung cancer ranked first and second worldwide, respectively. The section on thoracic neoplasms in the fifth edition of the WHO Classification of Tumors (6) recommends the use of an IHC package containing TTF-1 and P40 as specific markers to diagnose adenocarcinoma and squamous cell carcinoma, respectively, in NSCLC biopsy tissues without distinct morphological differentiation of adenocarcinoma and squamous cell carcinoma. However, no clear definition or explanation has been provided for the double expression of P40 and TTF-1 markers in NSCLC. Following the first case reported by Pelosi *et al* (1), only six additional cases have been reported, including the current case (2-5). To the best of our knowledge, the present study reports the first-ever case of NSCLC with EML4-ALK and PIK3CA gene mutations. The clinicopathological and molecular characteristics of this disease were analyzed using methods documented in the literature. The clinical features of all the reported cases are presented in Table I. A total of seven cases have been investigated. The tumor has mostly affected

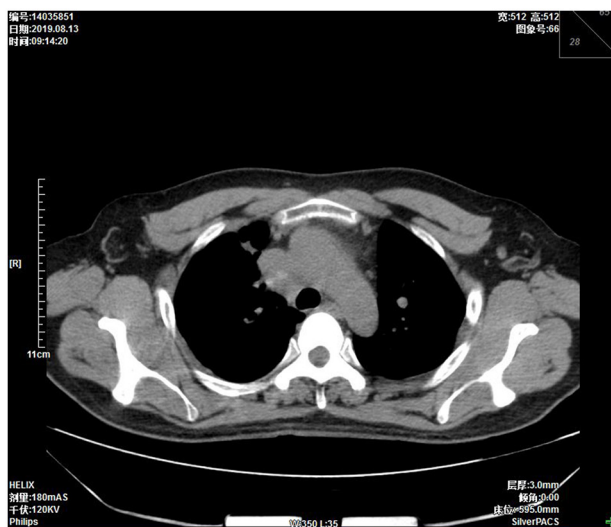


Figure 8. After 1 month of treatment, computed tomography showed that the maximum diameter of the right upper mediastinal mass had been reduced by approximately half.

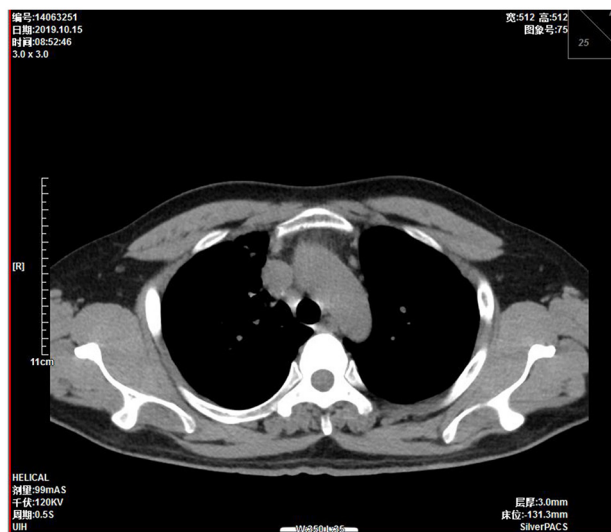


Figure 9. Three months after treatment, computed tomography showed that the maximum diameter of the right upper mediastinal mass was reduced by more than half.

males (male to female ratio, 5:2). The age range of the patients is 38-77 (median, 62; mean, 59.6) years, and six of the seven cases reported a history of smoking. A symptomatic cough and expectoration were present in one case, and a persistent headache was reported in one case in which the lung cancer was accompanied by brain metastasis. Lung tumors were found by CT examination in 3 patients. The symptoms of the remaining two cases remains unknown. The cancer was located in the left lobe in four cases and in the right lobe in three cases. The maximum diameter of the tumor was 1.9-8.5 cm. The thorax, liver, bone, brain and other sites were associated with pleural effusion in one case. CT scanning revealed no particular difference between these lung tumors and other cancers.

Several specimens were obtained for the analysis of pathological features, including bronchial biopsy, lung tumor puncture, lymph node puncture and lobectomy specimens.

The findings of the microscopic examination were not unusual compared with those of other lung cancer biopsies, punctures and surgical specimens. On microscopic observation, the high-grade tumor cells showed a solid nested patchy distribution, conspicuous atypia, high nucleoplasmic ratio and mitotic figures in all cells, and necrosis was present in some cases. These features were sometimes accompanied by squamous differentiation, glandular differentiation and peripheral palisading.

Pelosi *et al* (1,4) performed an electron microscopic examination of three cases, which revealed adenoid and squamous differentiation concurrently in the same tumor cells, which included abundant perinuclear stress fibers, cytoplasmic dense keratin fiber bundles and desmosomal junctions. The features of adenoid differentiation included the formation of extra-cellular lumen, villous cytoplasmic processes and mucous granules. The IHC results revealed that the same tumor cells co-expressed TTF-1 and P40 in all cases.

With regard to molecular genetic characteristics, no specific pattern in gene mutations was observed in these cases. Six cases had a TP53 mutation or polymorphism, but no TP53 mutation was detected in the current case. EGFR, KRAS, PTEN and NF1 mutations, and FGFR1 amplification with PD-L1 expression were also detected in certain cases. EML4-ALK and PIK3CA gene mutations were concurrently observed in the present case. ALK is a powerful tumor driver gene. In NSCLC, 3-7% of cases have ALK fusion mutations (8), of which EML4-ALK fusion mutations are the most common, with >20 fusion configurations. EML4 exon 13-ALK exon 20 is the most common EML4-ALK fusion mutation, constituting ~50% of all mutations (9). Most fusion breakpoints occur within or upstream of exon 20 in the ALK gene, although a few occur in exon 19, enabling the fused ALK protein to retain an intact kinase region, a key site of carcinogenic activity. PIK3CA, a common proto-oncogene, occurs in 1-3% of lung cancers (10). Most mutations of the PIK3CA gene occur in exons 10 and 21, which encode the helical and kinase domains of the protein, respectively. PIK3CA gene mutation can activate different downstream signaling pathways, including AKT and mTOR pathways, thereby promoting the occurrence and development of tumors. As indicated by clinical analyses, PIK3CA mutation is an important mechanism of secondary resistance to EGFR-tyrosine kinase drugs in lung cancer (11). In the present case, the fusion configuration EML4 exon 6-ALK exon 20 had a mutation proportion of 24.77%. Cancers with this rare mutation are sensitive to treatment with crizotinib. PIK3CA mutations (4.32%) were also detected, for which no drug sensitivity is known, and resistance to gefitinib, erlotinib, afatinib and icotinib is recorded. EGFR mutation, which is most commonly found in patients with NSCLC, especially adenocarcinoma, was found in a previous case. The mutation leads to a change in normal cell biology that results in cancer (12).

No mutations in BRAF, HER2, KRAS, MET, ROS1, RET and NRAS genes were detected in the present case. BRAF-encoded RAF kinase is a key regulator of the MAPK/ERK pathway, and its mutation can lead to the continuous activation of RAF protein, resulting in uncontrolled cell growth and proliferation (13). HER2 mutations occur in ~3% of cases of NSCLC. HER2 is a member of the EGFR family; it

Table I. Clinicopathologic information of the seven known cases of P40 and TTF-1 expression in non-small cell lung cancer.

First author/s, year	Sex/age (years)	Smoker (Y/N)	Site	Maximum diameter (cm)	Pleural effusion (Y/N)	IHC findings	Electron microscopy findings	Tumor stage	Therapy	Clinical outcome (Refs.)
Pelosi <i>et al</i> , 2015	M/77	Y	Left lung, hilar mass	8.5	Y	P40+ and TTF-1+ in most tumor cells	Characteristics of glandular and squamous differentiation	c-IVA	None	DOD 1.5 months (1)
Hayashi <i>et al</i> , 2018	M/73	Y	Left lung lobe	1.9	N	P40+ and TTF-1+ in most tumor cells, CD56 focal+, napsin-, CK5/6-, Syn-, CgA- and Ki-67 (40%)	None	NA	LC	NA (2)
Spinelli <i>et al</i> , 2019	M/51	Y	Right upper lobe	3.1	N	P40+ and TTF-1+ in most tumor cells	None	c-IVB	RT and CT	Fast progress, no specific details (3)
Pelosi <i>et al</i> , 2021	W/62	Y	Upper right lobe	4.5	N	P40+ and TTF-1+ in most tumor cells	Characteristics of glandular and squamous differentiation	IIIB	LC + CT + TT	DOD 48 months (4)
Pelosi <i>et al</i> , 2021	M/62	Y	Left lower lobe	4.7	N	P40+ and TTF-1+ in most tumor cells	Characteristics of glandular and squamous differentiation	yIIIA	LC + CT + TT	DOD 3 months (4)
Chen and Cheng, 2022	F/54	Y	Center of lower left lobe	2.2	N	P40+, TTF-1+,	None	NA	None	9 mo Lost to follow-up (5)
Present study	M/38	N	Right mediastinum	4.5	N	P40 (50-60%), TTF-1+, P53-, P63-, CK7+, CD56-, napsin A+, CK5/6-, Syn-, CgA- and Ki-67 (10%)	None	c-IVB	CT + TT	3 mo Lost to follow-up -

TTF-1, thyroid transcription factor-1; Y, yes; N, no; M, male; F, female; IHC, immunohistochemistry; CK, cytokeratin; Syn, synaptophysin; CgA, chromogranin A; NA, not available; LC, lobectomy; RT, radiotherapy; CT, chemotherapy; TT, targeted therapy; DOD, died of disease.

is a receptor tyrosine kinase that is bound to the surface of cell membranes and regulates various signal transduction pathways to promote cell growth and differentiation. Mutations in HER2 cause abnormal cell growth and differentiation (14). The KRAS gene is mutated in 20-30% of cases of NSCLC, and these mutations lead to uncontrolled malignant cell proliferation and division (15). MET is a proto-oncogene. The MET gene encodes a transmembrane receptor protein with tyrosine kinase activity, which can affect cell growth, survival, invasion, metastasis and angiogenesis. The mutation of MET is known to cause excessive cell proliferation (16). ROS1 mutation can produce an ROS1 fusion protein in which the ROS1 tyrosine kinase is continuously activated and induces downstream signaling, resulting in excessive cell growth and proliferation (17). The mutation probability of the NRAS gene in NSCLC is ~1%. The NRAS protein encoded by the NRAS gene operates within the RAS/MAPK signaling pathway, and its mutation can lead to continuous activation of the NRAS protein, causing uncontrolled cell proliferation (18).

Hypotheses for the causes of such lesions have been disclosed in previous studies. Specifically, Pelosi *et al* (1) proposed that the double expression of P40 and TTF-1 may be caused by stem/progenitor cell plasticity. In another study, it was suggested that the common mutation of TP53 and PTEN alleles leads to poorly differentiated and multiphenotypic tumors (2). Pelosi *et al* (4) also suggested that this tumor may be derived from the co-differentiation of distal bronchial basal stem cells with the double-positive expression of adenosquamous markers. The present case had no TP53 mutations, which supports the third hypothesis. Such lesions are not distinctly classified in the fifth edition of the WHO Classification of Tumors. Multiple names for adenosquamous carcinoma have been proposed, including NSCLC-not otherwise specified, NSCLC with adenosquamous cell immunophenotype, and NSCLC with the double expression of adenocarcinoma and squamous cell carcinoma markers. Based on the observation of the tumor cells using electron microscopy, which revealed that three cases had characteristics of glandular and squamous differentiation, and the detection of seven cases with the concurrent expression of glandular and squamous markers by IHC, an appropriately named adenosquamous carcinoma is likely to be accepted. The current authors propose that the WHO term adenosquamous carcinoma (6) should be renamed as compound carcinoma, defined as squamous carcinoma and adenocarcinoma, each $\geq 10\%$. This suggestion is similar to the concept of compound small cell carcinoma (6), which is considered as small cell carcinoma plus any NSCLC, adenocarcinoma, squamous cell carcinoma or large cell carcinoma.

Treatments used for this cancer include surgery, radiotherapy, chemotherapy and targeted therapy. Three patients died during follow-up, and the survival time ranged from 1.5 to 48.0 months (mean, 17.5 months). In the present case, the tumor size shrank remarkably after 3 months of chemotherapy plus targeted therapy, but the patient was lost to further follow-up.

Overall, this type of NSCLC with concurrent P40 and TTF-1 expression presents several unique clinicopathological features. This cancer is not yet mentioned in the guidelines of the WHO Classification of Tumors, the International Association for the Study of Lung Cancer, or other authoritative organizations. For consideration as an independent subtype,

the clinicopathological characteristics, molecular phenotype, treatment and prognosis of NSCLC with concurrent P40 and TTF-1 expression warrant further studies and investigation.

Acknowledgements

Not applicable.

Funding

No funding was received.

Availability of data and materials

The datasets used and/or analyzed during the current study are available from the corresponding author on reasonable request.

Authors' contributions

YC and BH conceived the study and drafted the manuscript. HL and XC were responsible for the collection and analysis of case data and literature. BH and JY interpreted the data and revised the manuscript. YC and HL confirm the authenticity of all the raw data. All authors agreed on the journal to which the article has been submitted and have agreed to be accountable for all aspects of the work. All authors read and approved the final version of the manuscript.

Ethics approval and consent to participate

Not applicable.

Patient consent for publication

As the patient was lost to follow-up, a waiver of patient consent for publication was provided by the Ethics Committee of The First People's Hospital of Xiaoshan District (Hangzhou, China).

Competing interests

The authors declare that they have no competing interests.

References

1. Pelosi G, Fabbri A, Tamborini E, Perrone F, Testi AM, Settanni G, Busico A, Centonze G, Braidotti P, Bulfamante G, *et al*: Challenging lung carcinoma with coexistent Δ Np63/p40 and thyroid transcription factor-1 labeling within the same individual tumor cells. *J Thorac Oncol* 10: 1500-1502, 2015.
2. Hayashi T, Takamochi K, Yanai Y, Mitani K, Tomita H, Mogushi K, Suehara Y, Takahashi F, Suzuki K, Saito T and Yao T: Non-small cell lung carcinoma with diffuse coexpression of thyroid transcription factor-1 and Δ Np63/p40. *Hum Pathol* 78: 177-181, 2018.
3. Spinelli M, Khorshad J and Viola P: When tumor doesn't read textbook. Third case of TTF1 and p40 co-expression in the same tumour cells in a non-small cell carcinoma. A potential new entity to consider? *Pathologica* 111: 58-61, 2019.
4. Pelosi G, Bulloni M, Martina Vescio M, Uccella S, Forest F, Leone G, Barberis M, Rahal D, Bossi P, Finzi G, *et al*: Coexpression of Δ Np63/p40 and TTF1 within most of the same individual cells identifies life threatening NSCLC featuring squamous and glandular biphenotypic differentiation: Clinicopathologic correlations. *JTO Clin Res Rep* 2: 100222, 2021.

5. Chen B and Cheng N: Coexpression of thyroid transcription factor 1 and P40 in non-small cell lung cancer cells: A case report. *Chin J Pathol* 51: 558-560, 2022 (In Chinese).
6. WHO Classification of Tumours Editorial Board: WHO classification of tumours. Thoracic Tumours. 5th edition. IARC Press, Lyon, 2021.
7. Sung H, Ferlay J, Siegel RL, Laversanne M, Soerjomataram I, Jemal A and Bray F: Global cancer statistics 2020: GLOBOCAN estimates of incidence and mortality worldwide for 36 cancers in 185 countries. *CA Cancer J Clin* 71: 209-249, 2021.
8. Shi Y, Au JSK, Thongprasert S, Srinivasan S, Tsai CM, Khoa MT, Heeroma K, Itoh Y, Cornelio G and Yang PC: A prospective, molecular epidemiology study of EGFR mutations in Asian patients with advanced non-small-cell lung cancer of adenocarcinoma histology (PIONEER). *J Thorac Oncol* 9: 154-162, 2014.
9. Pillai RN and Ramalingam SS: The biology and clinical features of non-small cell lung cancers with EML4-ALK translocation. *Curr Oncol Rep* 14: 105-110, 2012.
10. Samuels Y, Wang Z, Bardelli A, Silliman N, Ptak J, Szabo S, Yan H, Gazdar A, Powell SM, Riggins GJ, *et al*: High frequency of mutations of the PIK3CA gene in human cancers. *Science* 304: 554, 2004.
11. Sequist LV, Waltman BA, Dias-Santagata D, Digumarthy S, Turke AB, Fidias P, Bergethon K, Shaw AT, Gettinger S, Cosper AK, *et al*: Genotypic and histological evolution of lung cancers acquiring resistance to EGFR inhibitors. *Sci Transl Med* 3: 75ra26, 2011.
12. Parra HS, Cavina R, Latteri F, Zucali PA, Campagnoli E, Morengi E, Grimaldi GC, Roncalli M and Santoro A: Analysis of epidermal growth factor receptor expression as a predictive factor for response to gefitinib ('Iressa', ZD1839) in non-small-cell lung cancer. *Br J Cancer* 91: 208-212, 2004.
13. Dalle S, Poulalhon N and Thomas L: Vemurafenib in melanoma with BRAF V600E mutation. *N Engl J Med* 365: 1448-1449, 2011.
14. Arcila ME, Chaft JE, Nafa K, Roy-Chowdhuri S, Lau C, Zaidinski M, Paik PK, Zakowski MF, Kris MG and Ladanyi M: Prevalence, clinicopathologic associations, and molecular spectrum of ERBB2 (HER2) tyrosine kinase mutations in lung adenocarcinomas. *Clin Cancer Res* 18: 4910-4918, 2012.
15. Benvenuti S, Sartore-Bianchi A, Di Nicolantonio F, Zanon C, Moroni M, Veronese S, Siena S and Bardelli A: Oncogenic activation of the RAS/RAF signaling pathway impairs the response of metastatic colorectal cancers to anti-epidermal growth factor receptor antibody therapies. *Cancer Res* 67: 2643-2648, 2007.
16. Schwab R, Petak I, Kollar M, Pinter F, Varkondi E, Kohanka A, Barti-Juhasz H, Schönleber J, Brauswetter D, Kopper L and Urban L: Major partial response to crizotinib, a dual MET/ALK inhibitor, in a squamous cell lung (SCC) carcinoma patient with de novo c-MET amplification in the absence of ALK rearrangement. *Lung Cancer* 83: 109-111, 2014.
17. Shaw AT and Solomon BJ: Crizotinib in ROS1-rearranged non-small-cell lung cancer. *N Engl J Med* 372: 683-684, 2015.
18. Dumaz N: Mechanism of RAF isoform switching induced by oncogenic RAS in melanoma. *Small GTPases* 2: 289-292, 2011.



This work is licensed under a Creative Commons Attribution-NonCommercial-NoDerivatives 4.0 International (CC BY-NC-ND 4.0) License.